

UC Davis

UC Davis Previously Published Works

Title

A Freely Soluble, High Electron Affinity Molecular Dopant for Solution Processing of Organic Semiconductors

Permalink

<https://escholarship.org/uc/item/5bm0x4km>

Journal

Chemistry of Materials, 31(5)

ISSN

0897-4756

Authors

Saska, Jan
Gonel, Goktug
Bedolla-Valdez, Zaira I
[et al.](#)

Publication Date

2019-03-12

DOI

10.1021/acs.chemmater.8b04150

Peer reviewed

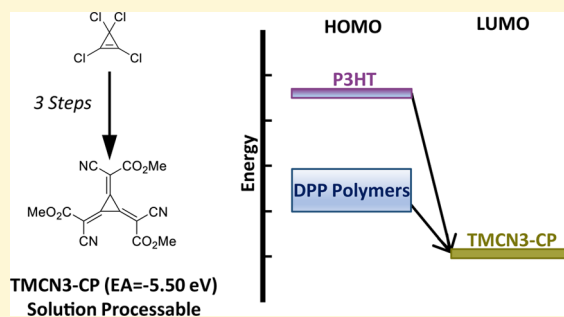
1 A Freely Soluble High Electron Affinity Molecular Dopant for 2 Solution Processing of Organic Semiconductors

3 Jan Saska,[†] Goktug Gonenl,[§] Zaira I. Bedolla-Valdez,[§] Sean D. Aronow,[†] Nikolay E. Shevchenko,[†]
4 Alexander S. Dudnik,^{†,‡} Adam J. Moulé,^{*,§} and Mark Mascal^{*,†,‡}

5 [†]Department of Chemistry and [§]Department of Chemical Engineering, University of California, Davis, California 95616, United
6 States

7 **S** Supporting Information

8 **ABSTRACT:** Molecular dopants are increasingly studied to enhance
9 the conductivity of semiconducting polymers. Most available p-type
10 dopants have low solubility in common solvents and moderate
11 electron affinities (EA), which makes solution processing difficult and
12 limits the range of semiconducting polymers that can be doped. Here,
13 we describe the synthesis and characterization of the new molecular
14 dopant TMCN3-CP, which has an EA of -5.5 eV. We show that high
15 ionization energy alternating copolymers such as PDPP-4T, PDPP-
16 3T, and PDPP-T-TT-T can be p-type doped and achieve high
17 conductivities with TMCN6-CP using sequential solution processing.
18 The main advantage of this new dopant is the ability to chemically
19 tailor the ester groups, which we demonstrate here for sequential
20 solution doping of films. Sequential solution processing allows a greater ability to control the film morphology and is also
21 desirable for scale-up to large-area polymer electronics.



22 ■ INTRODUCTION

23 Stimulated by the continual drive for innovation in micro-
24 electronics, the development of organic semiconductors
25 (OSCs) as the basis for solution-processable organic field-
26 effect transistors (OFETs) has become a major field of
27 research, most of which focuses on the development of
28 polymeric and molecular p-type, or hole-transporting, organic
29 materials.^{1,2} Due to their low cost, light weight, flexibility, and
30 low environmental footprint,^{3–5} OSCs are particularly useful
31 for applications such as flexible displays,⁶ chemical sensors,⁵
32 and organic photovoltaics.⁷

33 Molecular p-type dopants are relatively small neutral organic
34 species with high electron affinities that can accept electrons
35 from OSCs, leading to an increase in the number of free
36 charges, which results in multiple orders of magnitude
37 increases in conductivity.^{8,9} As the range of OSCs broadens
38 both in structure and electronic properties, a new generation of
39 dopants has been developed to improve the performance of the
40 devices derived therefrom.

41 Currently, the most widely studied and used organic dopant
42 is 2,3,5,6-tetrafluoro-7,7,8,8-tetracyanoquinodimethane
43 (F4TCNQ).¹⁰ Indeed, a search of the *Chemical Abstracts*
44 database finds nearly 2000 journal articles and patents in which
45 F4TCNQ appears in one context or another. A major
46 challenge however has been to develop dopants that keep
47 pace with the decreasing HOMO energy levels of higher
48 performance materials. F4TCNQ has a measured electron
49 affinity (EA) of -5.24 eV,¹⁰ which is adequate in combination
50 with relatively electron-rich polymers such as poly(3-

hexylthiophene) (P3HT).^{11,12} However, more advanced
51 OSCs tend toward higher ionization energies,^{2,13–15} and
52 many cannot therefore be effectively doped with F4TCNQ.
53 This fact has led to a growing interest in dopants with ultralow
54 LUMO energies, and the past decade has seen reports of the
55 synthesis of 1,3,4,5,7,8-hexafluorotetracyanonaphthoquinodi-
56 methane (F6-TCNNQ; EA = -5.37 eV),¹⁶ 3,6-difluoro-
57 2,5,7,7,8,8-hexacyanoquinodimethane (F2-HCNQ; EA =
58 -5.59 eV),¹⁷ and molybdenum tris(1,2-bis(trifluoromethyl-
59)ethane-1,2-dithiolenyl) [Mo(tfd)₃, EA = -5.60 eV].¹⁸ The
60 strongest molecular dopant to date is hexacyanotrimethylene-
61 cyclopropane (CN6-CP, EA = -5.87 eV), as reported by
62 Karpov et al.,¹⁹ although its original synthesis dates back to the
63 1970s.^{20–22}

64 Yet another hurdle is to identify dopants that enable the
65 application of solution processing of semiconducting polymers,
66 such as spin coating, screen printing, and inkjet printing.²³
67 Unfortunately, all of the above described dopants generally
68 suffer from poor solubility in common organic solvents. As a
69 result, they have to be introduced into OSCs either by
70 evaporation processes^{10,24} or premixing in an inert matrix.^{25,26}
71 This restricts development of technologies to mass-produce
72 organic electronics, which depends on solution processing.^{8,23}
73 In an effort to address this problem, Marder et al. reported the
74 synthesis of molybdenum tris-(1-(methoxycarbonyl)-2- 75

Received: September 29, 2018

Revised: February 4, 2019

76 (trifluoromethyl)ethane-1,2-dithiolene) $[\text{Mo}(\text{tfd}-\text{CO}_2\text{Me})_3]$
 77 (Figure 1),^{27,28} an analogue of $\text{Mo}(\text{tfd})_3$ with solubility nearly

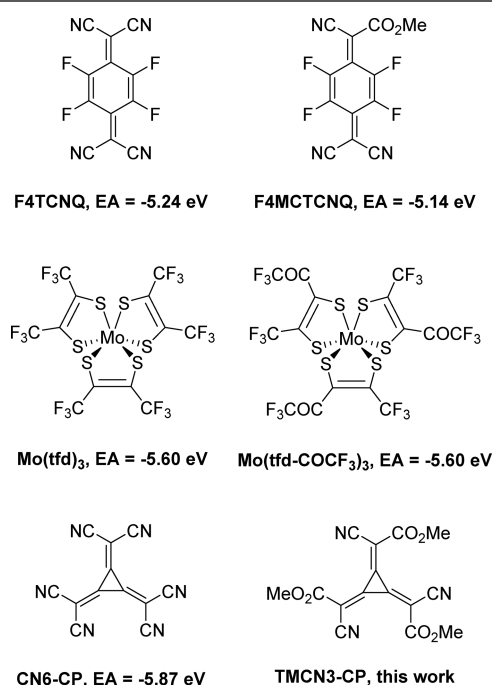


Figure 1. Structures of representative molecular dopants and their soluble analogues.

78 20 times higher, albeit at the cost of a dramatically reduced EA
 79 (5.00 eV). The same group has also reported molybdenum
 80 tris(1-(trifluoromethylcarbonyl)-2-(trifluoromethyl)-
 81 ethane-1,2-dithiolene) $[\text{Mo}(\text{tfd}-\text{COCF}_3)_3]$, which has a sol-
 82 ubility comparable to $\text{Mo}(\text{tfd}-\text{CO}_2\text{Me})_3$ and yet an EA
 83 equivalent to $\text{Mo}(\text{tfd})_3$.^{29,30} In our own approach,³¹ we
 84 prepared a series of F4TCNQ analogues wherein one or two
 85 of the nitrile functional groups were replaced with either
 86 methyl or octyl esters. It has been shown that these ester
 87 analogues exhibit an increase in solubility by a factor of up to
 88 100, while the EAs were only reduced by approximately 0.1 eV
 89 per ester group substituent. At the same time, it was observed
 90 that increased solubility leads to an increase in doping
 91 efficiency, such that higher conductivities in P3HT were
 92 achieved with F4MCTCNQ than F4TCNQ, despite the lower
 93 EA of the former.

94 Along with EA and solubility, a third issue in dopant design
 95 for organic electronic devices is control of the dopant diffusion
 96 and drift.^{8,32} In order for devices to be durable, dopants must
 97 remain in the domain in which they were printed and not
 98 diffuse or drift from their initial position. Volatile dopants like
 99 I₂ for example are particularly difficult to process because they
 100 sublime out of the polymer at room temperature.³³ We
 101 recently demonstrated that dopant diffusion, which has
 102 negative effects both on device performance and lifetime,^{34,35}
 103 is significantly reduced by the substitution of even one nitrile
 104 group in F4TCNQ for a methyl ester.³⁴

105 Applying the same molecular design principles, we now
 106 present a simple and efficient synthesis of the high EA soluble
 107 molecular dopant trimethyl 2,2',2''-(cyclopropane-1,2,3-triylidene)-tris(cyanoacetate) (TMCN3-CP), an analogue of CN6-CP in which three of the six nitrile groups are replaced with 108 methyl esters. Its electrochemical properties measured using

111 cyclic voltammetry (CV) are reported. Additionally, a series of
 112 polymer films were sequentially doped from solution to
 113 determine the changes that TMCN3-CP induced on the
 114 optical absorbance and conductivity of the films.

115 P3HT has a reported ionization energy of 4.4–5.1 eV,
 116 depending on the literature source.^{11,36,37} We also include in
 117 this study a series of alternating copolymers with diketopyrro-
 118 lo-pyrrole (DPP) groups that have higher ionization energies
 119 than P3HT and cannot be effectively p-doped by F4TCNQ.¹⁹
 120 Supporting Information Figure S1 gives the molecular
 121 structures of these polymers, and Supporting Information
 122 Figures S2–S4 show that the addition of F4TCNQ to DPP
 123 polymers does not change the absorbance spectrum, which is a
 124 clear demonstration that no polaron states are formed. The
 125 repeating units present a common DPP acceptor moiety with a
 126 donor unit consisting of three thiophenes (3T), four
 127 thiophenes (4T), or a thiophene-thienothiophene-thiophene
 128 (T-T-T-T).^{38,39} These three polymers were chosen because
 129 they have been well studied for OFET applications and have
 130 high reported hole mobilities.^{39,40} In addition, PDPP-4T and
 131 PDPP-T-T-T have been recently used to study the
 132 effectiveness of p-type dopants, including FeCl₃, Mo(tfd)₃,
 133 and Mo(tfd-CO₂Me)₃.⁴¹ PDPP-T-T-T was also used to
 134 study doping by F4TCNQ, F6TCNNQ, and CN6-CP.^{19,36} We
 135 show here that all three copolymers are effectively doped by
 136 sequential solution processing using TMCN3-CP. This is, to
 137 our knowledge, the first report of sequential solution doping of
 138 these high ionization energy polymers. In previous studies, the
 139 dopant was mixed into a batch solution for simultaneous
 140 deposition.^{19,36,41}

EXPERIMENTAL SECTION

142 **Materials.** CN6-CP⁻ was prepared according to the method
 143 published by Karpov et al.¹⁹ Nitrosonium tetrafluoroborate and
 144 tetrachlorocyclopropane were purchased from Acros Organics. All
 145 other reagents and solvents were purchased from Sigma-Aldrich and
 146 used as supplied. PDPP-T-T-T and PDPP-4T were purchased from
 147 Ossila. PDPP-3T was provided by the Dudnik group. P3HT was
 148 purchased from Sigma Aldrich (MW: 50000–70000, regioregularity
 149 ≥ 90%). F4TCNQ was purchased from Tokyo Chemical Industry
 150 Co., Ltd.

151 **Characterization.** ¹H and ¹³C NMR spectra were measured using
 152 a 400 MHz Bruker Nanobay AVIIIHD spectrometer in CDCl₃
 153 solvent. All chemical shifts (δ) are reported in parts per million
 154 (ppm) relative to chloroform residual solvent peaks (δ_H = 7.26 ppm,
 155 δ_C = 77.0 ppm).

156 Cyclic voltammograms (CVs) were recorded on a BASi Epsilon
 157 MF-9092 electrochemical workstation. Redox potentials were
 158 measured in degassed anhydrous acetonitrile solution containing
 159 tetramethylammonium tetrafluoroborate as a supporting electrolyte
 160 (0.05 M) using a platinum disk working electrode (φ = 1.6 mm), a
 161 glassy carbon counter electrode, and a Ag/AgCl reference electrode.
 162 The concentration of substrates in the working solution was 0.50 mM,
 163 and the electrochemical potential sweep rate was fixed at 100 mV/s.

164 High-resolution mass spectra (HRMS) were recorded on a Thermo
 165 Fisher Hybrid LTQ-Orbitrap XL mass spectrometer.

166 UV-vis-NIR spectra were measured using a PerkinElmer Lambda
 167 750 spectrometer. The glass substrates were sequentially cleaned in
 168 ultrasonic baths of acetone, methanol, isopropanol, and deionized
 169 water, followed by drying with nitrogen. The substrates were then
 170 exposed to UV/ozone for 30 min before use. Film samples were
 171 prepared by dissolving the polymers in chlorobenzene (CB) (for
 172 P3HT) or 1:1 CHCl₃/CB for DPP copolymers at a concentration of 3
 173 mg/mL. The samples were spin coated for film thicknesses of ~50
 174 nm. TMCN3-CP was dissolved in CH₂Cl₂ or 2:1 CH₂Cl₂/acetonitrile
 175 and sequentially coated onto the same substrate before spinning the

176 sample to remove excess solution. Film thicknesses were measured
177 with a Veeco Dektak 150 surface profilometer. All UV–vis–NIR
178 spectra were measured under ambient conditions in air except for the
179 time-dependent UV–vis–NIR experiments shown in Figures S9 and
180 S12. The two samples in these figures were sealed in a nitrogen-filled
181 glovebox (O_2 level < 10 ppm, H_2O level < 5 ppm) in a sample holder
182 that was designed by our group.⁴²

183 Conductivity measurements of doped films were performed with a
184 four-point probe setup on Si substrates using a Keithley 2450 source
185 measurement unit. Four electrodes (5 nm Cr/95 nm Au, $1 \times 5 \text{ mm}^2$,
186 1 mm spacing) were deposited through a shadow mask by thermal
187 evaporation. Neat films were measured using a two-wire probe with
188 10–20 μm channel length and 1–2 mm channel width. The same
189 procedure was used for substrate cleaning and sequential film
190 deposition as described above. All conductivity measurements were
191 performed in the dark under a nitrogen atmosphere in a glovebox.

192 **Synthesis of TMCN3-CP.** Potassium Trimethyl 2,2',2''-(Cyclo-
193 propane-1,2,3-triylidene)-tris(cyanoacetate) Radical Anion (**2**). To
194 a suspension of sodium hydride (850 mg of a 60% dispersion in
195 mineral oil, 21.2 mmol) in anhydrous 1,2-dimethoxyethane (9.0 mL)
196 at 0 °C was added methyl cyanoacetate (0.740 mL, 829 mg, 8.42
197 mmol), and the reaction mixture was stirred at rt for 1 h.
198 Tetrachlorocyclopropene **1** (0.360 mL, 522 mg, 2.95 mmol) was
199 added dropwise, and the mixture was stirred for a further 2 h during
200 which an orange precipitate formed. The precipitate was collected by
201 vacuum filtration, washed with Et_2O , and introduced in a single
202 portion into a solution of potassium persulfate (1.14 g, 4.20 mmol) in
203 water (50 mL). The resulting deep purple mixture was stirred at rt for
204 3 h during which a purple precipitate formed. This precipitate was
205 collected by vacuum filtration, washed with water ($\times 3$), and dried
206 under high vacuum for 16 h to give **2** (727 mg, 71%) as a purple
207 powder.

208 HRMS (ESI⁻) $C_{15}H_9N_3O_6^-$ [M]⁻ m/z calcd. 327.0491, found
209 327.0500; mp 242 °C (dec).

210 NMR spectra of **2** could not be obtained due to the open shell
211 nature of the compound.

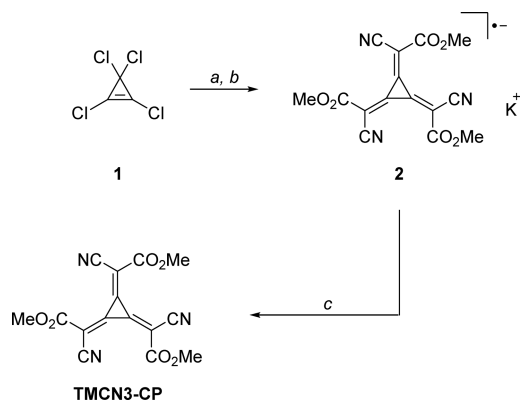
212 Trimethyl 2,2',2''-(Cyclopropane-1,2,3-triylidene)-tris-
213 (cyanoacetate) (TMCN3-CP). All operations were performed in a
214 glovebox under a dry nitrogen atmosphere. To a suspension of **2** (100
215 mg, 0.27 mmol) in anhydrous CH_2Cl_2 (1.0 mL) was added $NOBF_4$
216 (157 mg, 1.35 mmol), and the mixture was stirred for 30 min. The
217 solids were removed by filtration, and the filtrate was diluted with
218 hexane (50 mL). The resulting yellow precipitate was collected by
219 filtration and dried in a stream of nitrogen for 3 h to give TMCN3-CP
220 (64.0 mg, 72%).

221 ¹H NMR (400 MHz, $CDCl_3$) δ 4.08 (s, 3H); ¹³C NMR (101 MHz,
222 $CDCl_3$) δ 160.0, 128.6, 113.7, 103.8, 56.1; HRMS (ESI⁻)
223 $C_{15}H_9N_3O_6^-$ [M]⁻ m/z calcd. 327.0491, found 327.0500; mp 108
224 °C (dec).

225 ■ RESULTS AND DISCUSSION

226 **Synthesis of TMCN3-CP.** TMCN3-CP was prepared using
227 a modification of Karpov's protocol for synthesis of CN6-CP
228 (Scheme 1).¹⁹ To this end, tetrachlorocyclopropene **1** was
229 treated with methyl cyanoacetate in the presence of excess
230 sodium hydride to give the bis-sodium salt of TMCN3-CP²⁻,
231 which was immediately subjected to oxidation with an aqueous
232 solution of potassium persulfate to give the radical anion salt **2**
233 in good yield. While the radical anion salt of TMCN3-CP **2** is a
234 known compound,²² to the best of our knowledge, no
235 synthesis of the fully oxidized neutral molecule has been
236 reported to date. We have found this salt to be remarkably
237 stable and were able to prepare and store multigram quantities
238 of the material in air without it showing any signs of
239 deterioration. Next, a second one-electron oxidation was
240 performed using nitrosonium tetrafluoroborate. Any excess of
241 this poorly soluble oxidant could be simply removed from the
242 reaction mixture by filtration, and upon addition of hexane,

Scheme 1. Synthesis of TMCN3-CP⁴²



^aReagents and conditions: a. methyl cyanoacetate, NaH, DME, 3 h; b. $K_2S_2O_8$, H_2O , 3 h, 71% over 2 steps; c. $NOBF_4$, CH_2Cl_2 , 30 min, 72%.

243 pure TMCN3-CP precipitated out of solution as a yellow
244 powder. The assigned C_3 symmetric structure of TMCN3-CP
245 was confirmed by NMR. It is important to note that, unlike its
246 precursor **2**, TMCN3-CP is highly air- and moisture-sensitive,
247 and all stages of the final synthetic step should be carried out in
248 a glovebox using anhydrous solvents. Longer term storage of
249 TMCN3-CP is best achieved under vacuum.

250 **Dopant Characterization.** With sufficient quantities
251 (>200 mg) of TMCN3-CP in hand, we set out to identify
252 solvents in which it could be handled without decomposition.
253 As expected, TMCN3-CP reacted almost immediately with all
254 polar protic (MeOH) and most aprotic solvents (acetone,
255 DMSO, aromatics) to which it was subjected. Even dry MeCN
256 only had a 1–2 min window before some degree of
257 discoloration could be seen. We did, however, find TMCN3-
258 CP to be both readily soluble and stable over a period of
259 several hours in halogenated solvents including chloroform,
260 dichloromethane, and hexafluorobenzene. As a result, we were
261 able to perform full characterization and structural assignment
262 of the molecule using conventional NMR techniques.

263 To estimate the reduction potentials and, by extension, the
264 EA of this new dopant molecule, we conducted a series of CV
265 measurements (Figure 2). Predictably, we observe two
266 reversible one-electron reductions corresponding to formation
267 of TMCN3-CP⁻ and TMCN3-CP²⁻. These occur at $E_{red1} =$
268 0.78 V and $E_{red2} = 0.12$ V versus Ag/AgCl, respectively. 268

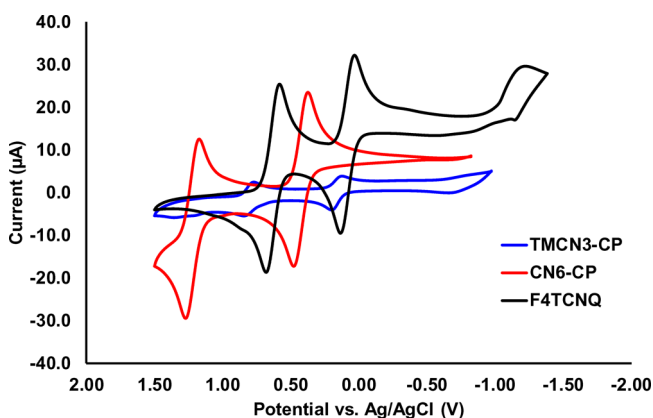


Figure 2. Cyclic voltammograms of TMCN3-CP, CN6-CP, and F4TCNQ.

269 According to the equation $E_{\text{LUMO}} = -e(E_{\text{red}} + E_{\text{ref}})$, where E_{ref}
 270 = 4.72 V for the Ag/AgCl reference electrode used in our
 271 measurements,¹² we calculate the LUMO levels for TMCN3-
 272 CP to be $E_{\text{LUMO1}} = -5.50$ eV and $E_{\text{LUMO2}} = -4.84$ eV.

273 The accuracy of these values was substantiated by
 274 conducting the same measurements on commercial
 275 F4TCNQ and CN6-CP⁻, which was prepared according to
 276 the literature method.¹⁹ The LUMO levels for both F4TCNQ
 277 ($E_{\text{LUMO1}} = -5.30$ eV) and CN6-CP ($E_{\text{LUMO1}} = -5.89$ eV)
 278 in excellent agreement with previously published values
 279 ($E_{\text{LUMO1}} = -5.33$ eV¹⁷ and $E_{\text{LUMO1}} = -5.87$ eV,¹⁹ respectively)
 280 based on CV measurements. All measured reduction potentials
 281 and calculated LUMO energy levels are summarized in Table
 282 1.

Table 1. Measured Reduction Potentials and Calculated LUMO Levels of TMCN3-CP, CN6-CP, and F4TCNQ

dopant	E_{red1} (V)	E_{LUMO1} (eV)	E_{red2} (V)	E_{LUMO2} (eV)
CN6-CP	1.17	-5.89	0.38	-5.10
TMCN3-CP	0.78	-5.50	0.12	-4.84
F4TCNQ	0.58	-5.30	0.03	-4.75

283 Figure 3 shows the UV-vis-NIR spectra of P3HT, PDPP-
 284 4T, PDPP-T-TT-T, and PDPP-3T that are doped by
 285 increasingly higher concentration solutions of TMCN3-CP.
 286 Sequential doping requires that the dopant solution be applied
 287 from a solvent that will not dissolve the polymer film. For the
 288 P3HT samples, all sequential doping was carried out in
 289 CH_2Cl_2 solution. For the DPP polymers, a 2:1 mixture of dry
 290 $\text{CH}_2\text{Cl}_2/\text{MeCN}$ was used to prevent dissolution of the
 291 polymer films.

292 Examination of the UV-vis-NIR spectra shows a decrease
 293 in the absorbance of the neutral polymer and a simultaneous
 294 absorbance increase below the neat polymer optical band gap.
 295 The absorbance for P3HT has previously been assigned as
 296 P3HT⁺ polaron absorbance in the range of 1–2 eV and
 297 centered at ~0.5 eV.^{43,44} For P3HT, almost all measurements
 298 have shown integer charge transfer with the exception of one
 299 report of a thermally unstable polymorph of P3HT with
 300 F4TCNQ.⁴⁵ Most alternating copolymers with strong acceptor
 301 groups exhibit only partial charge transfer when molecularly
 302 doped.⁴⁴ It was not the purpose of this work to assign a doping
 303 mechanism for the DPP polymers. We note instead that, with
 304 increasing TMCN3-CP concentration, the DPP copolymers all
 305 show increasing absorbance at ~0.88 eV and below the low
 306 energy side of the spectrum (<0.4 eV), consistent with
 307 previously reported p-doping by CN6-CP.¹⁹ We also note that
 308 previous reports of the doping of PDPP-T-TT-T by
 309 F6TCNNQ did not have a similar absorption change and
 310 partial charge transfer was determined.³⁶

311 Sequential doping is described by an equilibrium between
 312 dopants in the solution and film.²⁶ The driving force for charge
 313 transfer from the polymer to the dopant is ΔG for the reaction
 314 $\text{dopant}_{\text{solution}} + \text{polymer}_{\text{film}} \rightleftharpoons \text{dopant}_{\text{film}} + \text{polymer}_{\text{film}}^+$ and
 315 can be approximated by $\text{HOMO}_{\text{polymer}} - \text{LUMO}_{\text{dopant}}$. Dopants
 316 occupy sites on the polymer according to a Langmuir isotherm
 317 model given by

$$C_{\text{d,sat}} - C_{\text{d}} = \frac{K_{\text{eq}} C_{\text{s}}}{1 + K_{\text{eq}} C_{\text{s}}} \quad (1)$$

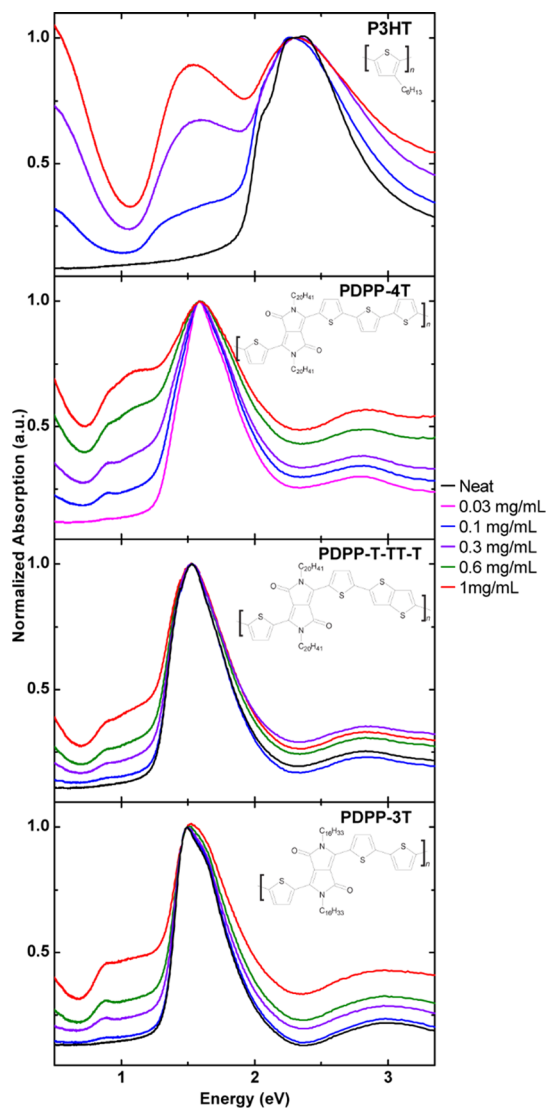


Figure 3. UV-vis-NIR spectra of P3HT, PDPP-4T, PDPP-T-TT-T, and PDPP-3T sequentially doped by solutions of TMCN3-CP. All measurements are normalized to the neat polymer absorbance maximum.

where C_{d} is the polaron concentration in the film, $C_{\text{d,sat}}$ is the total concentration of sites that could be doped from a solution at infinite concentration, C_{s} is the concentration of the dopant in solution, and K_{eq} is the equilibrium constant determined from ΔG .²⁶

It has often been reported that the efficiency of free charge creation from molecular doping is much less than unity.^{9,43,46} UV-vis-NIR cannot measure the creation of free charges but does give a measure of C_{d} in the polymer. In Supporting Information Figure S5, we show the change in the ratio of absorbance at the peak of the polaron state (1.52 eV for P3HT and 0.88 for all DPP polymers) compared to the absorbance maximum of the neutral polymer. Thus, we measure $(A_{\text{doped}} - A_{\text{neutral}})_{\text{polaron_max}} / (A_{\text{neutral}})_{\text{neutral_max}}$ as a function of the doping solution concentration. The data show a high slope at low dopant concentrations of P3HT and PDPP-4T followed by a reduction in the slope with higher dopant concentrations. This follows the expected trend that polarons are created efficiently at low doping levels and as the Fermi level shifts towards the polymer HOMO, doping efficiency is reduced.⁴⁶ In contrast, 338

both PDPP-T-TT-T and PDPP-3T show a low and linear increase in polaron density with increased dopant concentration, which indicates that these polymers are more difficult to dope. The IE of the DPP polymers has been measured using ultraviolet photoelectron spectroscopy by several groups to be in the same range, that is, 5.17–5.40 eV, but the relative IE between polymers is not consistent.^{38–40} Given the dispersity of the measured IE values, we cannot assign the IE of these polymers directly or the ΔG for doping. Our results instead show that C_d is higher for this PDPP-4T sample than the other DPP polymers. This increased doping level could originate from either a lower IE or larger $C_{d,sat}$ afforded by increased solvent swelling. This work shows that the doping efficiency depends not just on the driving force for doping (ΔG) but also on the volume density of doping sites $C_{s,sat}$ and access to these sites via solvent infiltration into the swollen polymer. The effects of molecular weight, polymer orientation, and side chain length or branching are matters for separate study.

Figure 4 shows the four-wire conductivity (σ) for all polymer films plotted as a function of the concentration of

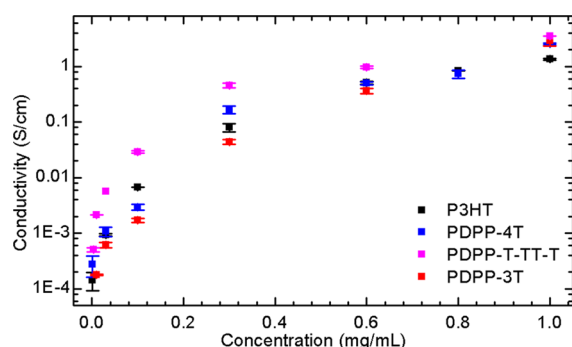


Figure 4. Four-wire conductivity measurements for P3HT, PDPP-4T, PDPP-T-TT-T, and PDPP-3T as a function of the TMCN3-CP sequential doping concentration.

TMCN3-CP used for sequential doping. The σ of all four films increases to above 1 S/cm² when sequentially doped from a solution of 1 mg/mL TMCN3-CP. The PDPP-T-TT-T film has the highest σ for all doping concentrations in spite of the fact that there are fewer polaron states than for P3HT or PDPP-4T. σ is a product of the density of mobile holes and the hole mobility (μ_h). PDPP-T-TT-T has the highest reported optimized μ_h of the three polymers at 5–10 cm²/(V·s).⁴⁷ The reported μ_h values for PDPP-4T, PDPP-3T, and P3HT are 0.5–1.5,⁴⁸ 0.5–2,^{38,40,49} and 0.1–0.3 cm²/(V·s),⁵⁰ respectively. All reported μ_h values were measured with field-effect transistors. Although C_d is lower in PDPP-T-TT-T, some combination of the high μ_h and/or a larger percentage of the polarons being free holes gives the highest σ for all doping concentrations. P3HT has much higher C_d but lower μ_h and/or free hole density and so has a similar σ value to the other polymers.

Comparing these results to other recent doping studies of DPP polymers, Liang et al. recently reported mixed batch σ measurements of PDPP-4T and PDPP-T-TT-T doped with FeCl₃ and Mo(tfd)₃.⁴¹ At all doping ratios, PDPP-4T showed higher conductivity for both dopants, which they attributed to a higher IE for PDPP-T-TT-T. The conductivity shown here is similar for PDPP-4T but higher for PDPP-T-TT-T. The comparison with this data does not mean that TMCN3-CP is a higher EA dopant than Mo(tfd)₃ because the samples were

prepared differently (batch vs sequential doping). The result does however clearly show that TMCN3-CP is more effective at doping PDPP-T-TT-T than Mo(tfd)₃ using solution methods, while both dopants have a similar ability to dope P3HT and PDPP-4T. Karpov et al. recently reported the doping of PDPP-T-TT-T and P3HT samples with F6TCNNQ³⁶ and CN6-CP.¹⁹ For PDPP-T-TT-T, doping with F6TCNNQ resulted in a σ of \sim 1 S/cm with a fairly low doping ratio but no increase with increased F6TCNNQ concentration. The conductivity of P3HT was higher when doped with F6TCNNQ.³⁶ Doping PDPP-T-TT-T with CN6-CP resulted in σ of almost 100 S/cm at a high doping ratio, which shows that higher EA dopants can yield greater increases in conductivity. To our knowledge, there are no other reports of molecular doping of PDPP-3T.

Lastly, we investigated the stability of doped polymer films. We performed sequential σ measurements over 7 days on TMCN3-CP- and F4TCNQ-doped P3HT films stored in four different environments. The samples were either kept under vacuum, in a glovebox filled with nitrogen ($O_2 < 10$ ppm and $H_2O < 5$ ppm), on a hot plate (60 °C) in the glovebox, and in air. Independent of the environment in which the samples were stored, the σ of all films decreased exponentially as shown in Figure S6, though the rate of σ decrease was lowest for the samples in the glovebox. We observed similar trends for conductivity of P3HT/F4TCNQ films to P3HT/TMCN3-CP films, as shown in Figure S7. It is important to note that organic molecular dopants have been shown to diffuse and drift in a polymer film.^{8,32,34} Since we made repeated conductivity measurements on the same films, it is likely that dopants drift away from the anode, which in turn decreases the conductivity.³² This indicates that the evaluation of the chemical stability of the dopants is not a simple matter of monitoring the conductivity.

An alternative probe of doping density over time is to measure the UV–vis–NIR spectra, which can resolve whether the decrease in conductivity is due to dopant drift or chemical degradation of the dopant. We thus monitor the UV–vis–NIR spectra for P3HT/TMCN3-CP and P3HT/F4TCNQ films stored in air and nitrogen continuously for 20 h. In Figures S8–S13, we track the changes in the peak of neutral P3HT absorbance (\sim 2.2 eV) and the P3HT⁺ polaron peak (1–2 eV). P3HT/TMCN3-CP films show a steady reduction in polaron density with time, with similar time constants for samples both in air and in a glovebox. This result suggests that the instability of the dopant in the film is not due to the reaction with O₂ or H₂O. We suspect, but cannot prove, a dimerization of the dopant radical anion similar to that observed for diester-substituted F4TCNQ.⁵¹ In contrast, P3HT/F4TCNQ films in nitrogen show no optical change, but films in air show a slow reduction in polaron states and an increase in neutral P3HT absorbance. F4TCNQ reacts with atmospheric O₂ and/or H₂O but shows long-time stability in N₂.

Since conductivity measurements cannot alone be used to determine dopant stability due to drift, the challenge will be to synthesize high EA dopants that are chemically stable, resistant to drift, and solution processable.

CONCLUSIONS

In conclusion, we describe the synthesis of TMCN3-CP, a new, solution processable, and thermally stable p-type dopant possessing three ester groups that allow the molecule to be chemically tailored. The high solubility and EA of TMCN3-CP

enable sequential molecular doping of a series of high IE conjugated polymers used in organic field-effect transistors. TMCN3-CP was added to the polymer films in a sequential solution processing step, resulting in clear p-type doping of P3HT, PDPP-4T, PDPP-T-TT-T, and PDPP-3T, whereas no polaron states were observed using F4TCNQ for the DPP-derived copolymers. At 1 mg/mL dopant concentration, all four polymers achieve conductivities of >1 S/cm. With lower dopant concentrations, the conductivity varied over a wider range, showing the need for in-depth studies of the effects of ionization energy and morphology on doping efficiency and the ratio between polarons and free holes. PDPP-T-TT-T polymer films exhibit lower conductivity when doped with TMCN3-CP than with CN6-CP but higher than with Mo(tfd)₃, FeCl₃, or F6TCNNQ. This study demonstrates the value of developing strong dopants with high solubilities. Further extension of this work will consider mono- and diester substitutions of CN6-CP, which should retain solubility but have even higher EA values than TMCN3-CP, and work along these lines will be reported in due course.

ASSOCIATED CONTENT

Supporting Information

The Supporting Information is available free of charge on the ACS Publications website at DOI: 10.1021/acs.chemmater.8b04150.

Molecular structures of all polymers used in this work; UV-vis-NIR curves of neat PDPP-4T, PDPP-T-TT-T, and PDPP-3T plotted with curves of the same polymer doped with F4TCNQ; plot of the ratio between the differential absorbance at the polaron maximum to the absorbance at the neutral polymer absorbance maximum for P3HT, PDPP-4T, PDPP-T-TT-T, and PDPP-3T doped with TMCN3-CP; ¹H-NMR spectrum of TMCN3-CP; ¹³C-NMR spectrum of TMCN3-CP (PDF)

AUTHOR INFORMATION

Corresponding Authors

*E-mail: amoule@ucdavis.edu (A.J.M.).

*E-mail: mjmascal@ucdavis.edu (M.M.).

ORCID

Alexander S. Dudnik: 0000-0001-9014-7660

Mark Maschal: 0000-0001-7841-253X

Notes

The authors declare no competing financial interest.

ACKNOWLEDGMENTS

This research was supported by the National Science Foundation grant 1636385. Z.I.B.-V. acknowledges the support of SENER CONACYT project 291145.

REFERENCES

- (1) Forrest, S. R. The Path to Ubiquitous and Low-Cost Organic Electronic Appliances on Plastic. *Nature* **2004**, *428*, 911–918.
- (2) Sirringhaus, H. 25th Anniversary Article: Organic Field-Effect Transistors: The Path Beyond Amorphous Silicon. *Adv. Mater.* **2014**, *26*, 1319–1335.
- (3) Günes, S.; Neugebauer, H.; Sariciftci, N. S. Conjugated Polymer-Based Organic Solar Cells. *Chem. Rev.* **2007**, *107*, 1324–1338.

- (4) Cheng, Y.-J.; Yang, S.-H.; Hsu, C.-S. Synthesis of Conjugated Polymers for Organic Solar Cell Applications. *Chem. Rev.* **2009**, *109*, 5868–5923.
- (5) Rim, Y. S.; Bae, S. H.; Chen, H.; De Marco, N.; Yang, Y. Recent Progress in Materials and Devices toward Printable and Flexible Sensors. *Adv. Mater.* **2016**, *28*, 4415–4440.
- (6) Gelinck, G. H.; Huitema, H. E. A.; van Veenendaal, E.; Cantatore, E.; Schrijnemakers, L.; van der Putten, J. B. P. H.; Geuns, T. C. T.; Beenhakkers, M.; Giesbers, J. B.; Huisman, B.-H.; Meijer, E. J.; Benito, E. M.; Touwslager, F. J.; Marsman, A. W.; van Rens, B. J. E.; de Leeuw, D. M. Flexible Active-Matrix Displays and Shift Registers Based on Solution-Processed Organic Transistors. *Nat. Mater.* **2004**, *3*, 106–110.
- (7) Mazzi, K. A.; Luscombe, C. K. The Future of Organic Photovoltaics. *Chem. Soc. Rev.* **2015**, *44*, 78–90.
- (8) Jacobs, I. E.; Moulé, A. J. Controlling Molecular Doping in Organic Semiconductors. *Adv. Mater.* **2017**, *29*, 1703063.
- (9) Lüssem, B.; Keum, C.-M.; Kasemann, D.; Naab, B.; Bao, Z.; Leo, K. Doped Organic Transistors. *Chem. Rev.* **2016**, *116*, 13714–13751.
- (10) Walzer, K.; Maennig, B.; Pfeiffer, M.; Leo, K. Highly Efficient Organic Devices Based on Electrically Doped Transport Layers. *Chem. Rev.* **2007**, *107*, 1233–1271.
- (11) Pingel, P.; Neher, D. Comprehensive Picture of p-Type Doping of P3HT with the Molecular Acceptor F₄TCNQ. *Phys. Rev. B* **2013**, *87*, 115209.
- (12) Pingel, P.; Schwarzl, R.; Neher, D. Effect of Molecular P-Doping on Hole Density and Mobility in Poly(3-Hexylthiophene). *Appl. Phys. Lett.* **2012**, *100*, 143303.
- (13) Chen, J.; Cao, Y. Development of Novel Conjugated Donor Polymers for High-Efficiency Bulk-Heterojunction Photovoltaic Devices. *Acc. Chem. Res.* **2009**, *42*, 1709–1718.
- (14) Wang, C.; Dong, H.; Hu, W.; Liu, Y.; Zhu, D. Semiconducting Π -Conjugated Systems in Field-Effect Transistors: A Material Odyssey of Organic Electronics. *Chem. Rev.* **2012**, *112*, 2208–2267.
- (15) Zaumseil, J.; Sirringhaus, H. Electron and Ambipolar Transport in Organic Field-Effect Transistors. *Chem. Rev.* **2007**, *107*, 1296–1323.
- (16) Koech, P. K.; Padmaperuma, A. B.; Wang, L.; Swensen, J. S.; Polikarpov, E.; Darsell, J. T.; Rainbolt, J. E.; Gaspar, D. J. Synthesis and Application of 1,3,4,5,7,8-Hexafluorotetracyanonaphthoquinodimethane (F6-TNAP): A Conductivity Dopant for Organic Light-Emitting Devices. *Chem. Mater.* **2010**, *22*, 3926–3932.
- (17) Gao, Z. Q.; Mi, B. X.; Xu, G. Z.; Wan, Y. Q.; Gong, M. L.; Cheah, K. W.; Chen, C. H. An Organic P-Type Dopant with High Thermal Stability for an Organic Semiconductor. *Chem. Commun.* **2008**, 117–119.
- (18) Qi, Y.; Sajoto, T.; Barlow, S.; Kim, E.-G.; Brédas, J.-L.; Marder, S. R.; Kahn, A. Use of a High Electron-Affinity Molybdenum Dithiolenes Complex to P-Dope Hole-Transport Layers. *J. Am. Chem. Soc.* **2009**, *131*, 12530–12531.
- (19) Karpov, Y.; Erdmann, T.; Raguzin, I.; Al-Hussein, M.; Binner, M.; Lappan, U.; Stamm, M.; Gerasimov, K. L.; Beryozkina, T.; Bakulev, V.; Anokhin, D. V.; Ivanov, D. A.; Günther, F.; Gemming, S.; Seifert, G.; Voit, B.; Di Pietro, R.; Kiriy, A. High Conductivity in Molecularly P-Doped Diketopyrrolopyrrole-Based Polymer: The Impact of a High Dopant Strength and Good Structural Order. *Adv. Mater.* **2016**, *28*, 6003–6010.
- (20) Fukunaga, T. Negatively Substituted Trimethylenecyclopropane Dianions. *J. Am. Chem. Soc.* **1976**, *98*, 610–611.
- (21) Fukunaga, T.; Gordon, M. D.; Krusic, P. J. Negatively Substituted Trimethylenecyclopropanes and Their Radical Anions. *J. Am. Chem. Soc.* **1976**, *98*, 611–613.
- (22) Fukunaga, T. Substituted Trimethylene Cyclopropanes, Salts, and Intermediates. U.S. Patent 4,003,943A, Jan 18, 1977.
- (23) Arias, A. C.; MacKenzie, J. D.; McCulloch, I.; Rivnay, J.; Salleo, A. Materials and Applications for Large Area Electronics: Solution-Based Approaches. *Chem. Rev.* **2010**, *110*, 3–24.
- (24) Scholes, D. T.; Hawks, S. A.; Yee, P. Y.; Wu, H.; Lindemuth, J. R.; Tolbert, S. H.; Schwartz, B. J. Overcoming Film Quality Issues for

- 572 Conjugated Polymers Doped with F4TCNQ by Solution Sequential
573 Processing: Hall Effect, Structural, and Optical Measurements. *J. Phys.*
574 *Chem. Lett.* **2015**, *6*, 4786–4793.
- 575 (25) Rainbolt, J. E.; Koech, P. K.; Polikarpov, E.; Swensen, J. S.;
576 Cosimbescu, L.; Von Ruden, A.; Wang, L.; Sapochak, L. S.;
577 Padmaperuma, A. B.; Gaspar, D. J. Synthesis and Characterization
578 of P-Type Conductivity Dopant 2-(3-(Adamantan-1-yl)Propyl)-3,5,6-
579 Trifluoro-7,7,8,8-Tetracyanoquinodimethane. *J. Mater. Chem. C* **2013**,
580 *1*, 1876–1884.
- 581 (26) Jacobs, I. E.; Aasen, E. W.; Oliveira, J. L.; Fonseca, T. N.;
582 Roehling, J. D.; Li, J.; Zhang, G.; Augustine, M. P.; Mascal, M.;
583 Moulé, A. J. Comparison of Solution-Mixed and Sequentially
584 Processed P3HT:F4TCNQ Films: Effect of Doping-Induced
585 Aggregation on Film Morphology. *J. Mater. Chem. C* **2016**, *4*,
586 3454–3466.
- 587 (27) Dai, A.; Wan, A.; Magee, C.; Zhang, Y.; Barlow, S.; Marder, S.
588 R.; Kahn, A. Investigation of P-Dopant Diffusion in Polymer Films
589 and Bulk Heterojunctions: Stable Spatially-Confined Doping for All-
590 Solution Processed Solar Cells. *Org. Electron.* **2015**, *23*, 151–157.
- 591 (28) Dai, A.; Zhou, Y.; Shu, A. L.; Mohapatra, S. K.; Wang, H.;
592 Fuentes-Hernandez, C.; Zhang, Y.; Barlow, S.; Loo, Y.-L.; Marder, S.
593 R.; Kippelen, B.; Kahn, A. Enhanced Charge-Carrier Injection and
594 Collection Via Lamination of Doped Polymer Layers P-Doped with a
595 Solution-Processible Molybdenum Complex. *Adv. Funct. Mater.* **2014**,
596 *24*, 2197–2204.
- 597 (29) Paniagua, S. A.; Baltazar, J.; Sojoudi, H.; Mohapatra, S. K.;
598 Zhang, S.; Henderson, C. L.; Graham, S.; Barlow, S.; Marder, S. R.
599 Production of Heavily N- and P-Doped Cvd Graphene with Solution-
600 Processed Redox-Active Metal–Organic Species. *Mater. Horiz.* **2014**,
601 *1*, 111–115.
- 602 (30) Mohapatra, S. K.; Zhang, Y.; Sandhu, B.; Fonari, M. S.;
603 Timofeeva, T. V.; Marder, S. R.; Barlow, S. Synthesis, Character-
604 ization, and Crystal Structures of Molybdenum Complexes of
605 Unsymmetrical Electron-Poor Dithiolenes Ligands. *Polyhedron* **2016**,
606 *116*, 88–95.
- 607 (31) Li, J.; Zhang, G.; Holm, D. M.; Jacobs, I. E.; Yin, B.; Stroeve, P.;
608 Mascal, M.; Moulé, A. J. Introducing Solubility Control for Improved
609 Organic P-Type Dopants. *Chem. Mater.* **2015**, *27*, 5765–5774.
- 610 (32) Müller, L.; Rhim, S.-Y.; Sivanesan, V.; Wang, D.; Hietzschold,
611 S.; Reiser, P.; Mankel, E.; Beck, S.; Barlow, S.; Marder, S. R.; Pucci, A.;
612 Kowalsky, W.; Lovrincic, R. Electric-Field-Controlled Dopant
613 Distribution in Organic Semiconductors. *Adv. Mater.* **2017**, *29*,
614 1701466.
- 615 (33) Heeger, Alan J.; Sariciftci, N. S.; Nardas, E. B. *Semiconducting*
616 *and Metallic Polymers*; Oxford University Press: Oxford, U.K., 2010.
- 617 (34) Li, J.; Koshnick, C.; Diallo, S. O.; Ackling, S.; Huang, D. M.;
618 Jacobs, I. E.; Harrelson, T. F.; Hong, K.; Zhang, G.; Beckett, J.;
619 Mascal, M.; Moulé, A. J. Quantitative Measurements of the
620 Temperature-Dependent Microscopic and Macroscopic Dynamics
621 of a Molecular Dopant in a Conjugated Polymer. *Macromolecules*
622 **2017**, *50*, 5476–5489.
- 623 (35) Zaikov, G. E.; Iordanskii, A. P.; Markin, V. S. *Diffusion of*
624 *Electrolytes in Polymers*; CRC Press: Utrecht, Netherlands, 1988.
- 625 (36) Karpov, Y.; Erdmann, T.; Stamm, M.; Lappan, U.; Guskova, O.;
626 Malanin, M.; Raguzin, I.; Beryozkina, T.; Bakulev, V.; Günther, F.;
627 Gemming, S.; Seifert, G.; Hamsch, M.; Mannsfeld, S.; Voit, B.; Kiriy,
628 A. Molecular Doping of a High Mobility Diketopyrrolopyrrole–
629 Dithienylthieno [3, 2-B] Thiophene Donor–Acceptor Copolymer
630 with F6TCNNQ. *Macromolecules* **2017**, *50*, 914–926.
- 631 (37) Fahlman, M.; Crispin, A.; Crispin, X.; Henze, S. K. M.; de Jong,
632 M. P.; Osikowicz, W.; Tengstedt, C.; Salaneck, W. R. Electronic
633 Structure of Hybrid Interfaces for Polymer-Based Electronics. *J. Phys.:*
634 *Condens. Matter* **2007**, *19*, 183202.
- 635 (38) Nielsen, C. B.; Turbiez, M.; McCulloch, I. Recent Advances in
636 the Development of Semiconducting Dpp-Containing Polymers for
637 Transistor Applications. *Adv. Mater.* **2013**, *25*, 1859–1880.
- 638 (39) Li, Y.; Sonar, P.; Murphy, L.; Hong, W. High Mobility
639 Diketopyrrolopyrrole (Dpp)-Based Organic Semiconductor Materials
for Organic Thin Film Transistors and Photovoltaics. *Energy Environ. Sci.* **2013**, *6*, 1684–1710.
- (40) Zhang, X.; Richter, L. J.; DeLongchamp, D. M.; Kline, R. J.;
Hammond, M. R.; McCulloch, I.; Heeney, M.; Ashraf, R. S.; Smith, J.
N.; Anthopoulos, T. D.; Schroeder, B.; Geerts, Y. H.; Fischer, D. A.;
Toney, M. F. Molecular Packing of High-Mobility Diketo Pyrrolo-
Pyrrole Polymer Semiconductors with Branched Alkyl Side Chains. *J.*
Am. Chem. Soc. **2011**, *133*, 15073–15084.
- (41) Liang, Z.; Zhang, Y.; Sourji, M.; Luo, X.; Boehm, A. M.; Li, R.;
Zhang, Y.; Wang, T.; Kim, D.-Y.; Mei, J.; Marder, S. R.; Graham, K. R.
Influence of Dopant Size and Electron Affinity on the Electrical
Conductivity and Thermoelectric Properties of a Series of Conjugated
Polymers. *J. Mater. Chem. A* **2018**, *6*, 16495–16505.
- (42) Jacobs, I. E.; Aasen, E. W.; Nowak, D.; Li, J.; Morrison, W.;
Roehling, J. D.; Augustine, M. P.; Moulé, A. J. Direct-Write Optical
Patterning of P3HT Films Beyond the Diffraction Limit. *Adv. Mater.*
2017, *29*, 1603221.
- (43) Salzmänn, I.; Heimel, G.; Oehzelt, M.; Winkler, S.; Koch, N.
Molecular Electrical Doping of Organic Semiconductors: Fundamen-
tal Mechanisms and Emerging Dopant Design Rules. *Acc. Chem. Res.*
2016, *49*, 370–378.
- (44) Ghani, F.; Opitz, A.; Pingel, P.; Heimel, G.; Salzmänn, I.;
Frisch, J.; Neher, D.; Tsami, A.; Scherf, U.; Koch, N. Charge Transfer
in and Conductivity of Molecularly Doped Thiophene-Based
Copolymers. *J. Polym. Sci., Part B: Polym. Phys.* **2015**, *53*, 58–63.
- (45) Jacobs, I. E.; Cendra, C.; Harrelson, T. F.; Bedolla Valdez, Z. I.;
Faller, R.; Salleo, A.; Moulé, A. J. Polymorphism Controls the Degree
of Charge Transfer in a Molecularly Doped Semiconducting Polymer.
Mater. Horiz. **2018**, *5*, 655–660.
- (46) Tietze, M. L.; Pahner, P.; Schmidt, K.; Leo, K.; Lüssem, B.
Doped Organic Semiconductors: Trap-Filling, Impurity Saturation,
and Reserve Regimes. *Adv. Funct. Mater.* **2015**, *25*, 2701–2707.
- (47) Li, J.; Zhao, Y.; Tan, H. S.; Guo, Y.; Di, C.-A.; Yu, G.; Liu, Y.;
Lin, M.; Lim, S. H.; Zhou, Y.; Su, H.; Ong, B. S. A Stable Solution-
Processed Polymer Semiconductor with Record High-Mobility for
Printed Transistors. *Sci. Rep.* **2012**, *2*, 754.
- (48) Ha, J. S.; Kim, K. H.; Choi, D. H. 2,5-Bis(2-octyldodecyl)-
pyrrolo[3,4-C]pyrrole-1,4-(2H,5H)-dione-Based Donor–Acceptor
Alternating Copolymer Bearing 5,5′-Di(thiophen-2-yl)-2,2′-biseleno-
phene Exhibiting 1.5 Cm²·V⁻¹·S⁻¹ Hole Mobility in Thin-Film
Transistors. *J. Am. Chem. Soc.* **2011**, *133*, 10364–10367.
- (49) Di Pietro, R.; Erdmann, T.; Carpenter, J. H.; Wang, N.;
Shivhare, R. R.; Formanek, P.; Heintze, C.; Voit, B.; Neher, D.; Ade,
H.; Kiriy, A. Synthesis of High-Crystallinity Dpp Polymers with
Balanced Electron and Hole Mobility. *Chem. Mater.* **2017**, *29*, 10220–
10232.
- (50) Noriega, R.; Rivnay, J.; Vandewal, K.; Koch, F. P. V.; Stingelin,
N.; Smith, P.; Toney, M. F.; Salleo, A. A General Relationship
between Disorder, Aggregation and Charge Transport in Conjugated
Polymers. *Nat. Mater.* **2013**, *12*, 1038–1044.
- (51) Li, J.; Holm, D. M.; Guda, S.; Bedolla-Valdez, Z. I.; Gonel, G.;
Jacobs, I. E.; Dettmann, M. A.; Saska, J.; Mascal, M.; Moulé, A. J.
Effect of Processing Conditions on Additive Disc Patterning of P3HT
Films. *J. Mater. Chem. C* **2019**, *7*, 302–313.